

# A First Principle Calculation of Electronic Structure of B and N Co-Doped Graphene: $\text{BNC}_2$ Hetero-Structure

Varsha Goyal<sup>1\*</sup>, Sabiha Khan<sup>2</sup>, Ritu Sharma<sup>3</sup>, Krishna Swaroop Sharma<sup>2</sup>

<sup>1</sup>Department of Chemical Science, The IIS University Jaipur

<sup>2</sup>Department of Physical Science, The IIS University Jaipur

<sup>3</sup>Department of Electronics & Communication, Malaviya National Institute of Technology Jaipur

## Abstract

Pure graphene is a zero gap 2D semi-metal with  $sp^2$  structure and a Dirac point at the Fermi level at symmetry point K. On doping graphene with electrons or holes a band gap opens, but it is associated with a shift of Dirac point, above the Fermi level for hole-doping and below the Fermi level for electron-doping. The co-doping of graphene with electrons and holes may therefore lead to a material for which the band gap may be obtained at the Fermi level. The new material may behave as a 2D semiconductor, suitable for device fabrication. In this paper the results of ab-initio calculation of electronic structure of graphene co-doped with 25 atomic % of B and an equal atomic % of N (i.e.,  $\text{BNC}_2$  hetero-structure) are presented. The gap opening in the new material is of the order of 1.0 eV, which is of the same order as that of Si. P-type character of this material is also revealed by the position of Fermi level, which is found to be slightly below the center of the gap and can be controlled by relative doping of B and N atoms in graphene.

**Keywords:** Density functional theory, Electronic structure calculations, Graphene, Nano-materials, 2D Semiconductor

## Introduction

Discovered by Novoselov *et al* (2004), the graphene is a 2D honey comb lattice, in which carbon atoms are bonded in  $sp^2$  structure. The graphene is a zero band gap material with its valence band and conduction band meeting on the Fermi level at the symmetry point K. This point is called Dirac point because of linear relationship between energy and momentum in the vicinity of this point, where the electrons behave as massless particles and obey Dirac's relativistic equation. The importance of graphene is now well established by its excellent properties and the applications to which it has been put or is in the process of development. These include: super capacitors, lithium ion batteries, fuels cells, solar cells, electrochemical sensors, bio-sensors, pesticide sensors, water purification etc. and for energy applications (Choi *et al.*, 2012; Ramchandran *et al.*, 2013; Liu *et al.*, 2012; Zhu *et al.*, 2014). However, zero band gap in pristine graphene makes it unsuitable for most of the electronic applications, as it would be difficult to switch off such a device.

Some of the recent investigations (Guo *et al.*, 2011; Tokarev *et al.*, 2015; Wang *et al.*, 2012; Fujimoto, 2015; Panchakarla *et al.*, 2009; Joucken *et al.*, 2012; Rani and Jindal, 2013) on graphene, reveal that an energy gap opens in the otherwise a zero gap semi-metal in pure state, on doping it with holes or electrons, making it suitable for switching action. But opening of energy gap in hole/electron doped

graphene is associated with shifting of the Dirac point, i.e., the centre of the energy gap opened in the doped graphene is displaced from the Fermi level. This shift is found to be above the Fermi level for hole-doping and below the Fermi level for electron-doping. As a result of it, such materials are not suitable for fabrication of electronic devices.

In a recent investigation, Sharma *et al* (2017) on using B and N respectively for hole and electron doping in graphene, observed that the shifting of Dirac point (i.e., the center of the energy gap in doped graphene) is almost equal in magnitude but opposite in direction for the two cases, when doping level was kept 25 atomic % in each case. Therefore, it may be concluded that by co-doping of graphene with B and N, it should be possible to obtain the energy band gap at the Fermi level, making it a suitable material for fabrication of electronic devices. Such devices shall be more efficient as compared to Si-based devices, on account of better electrical conductivity in graphene. The graphene based 2D electronics, therefore, has the scope for replacing Si-based 3D electronics in times to come.

Co-doping of graphene with B and N is a subject of current research. Some of the important experimental and theoretical investigations on the subject, reported in literature are as follows:

Jiang *et al* (2016) have studied role of B-doped, N-doped and co-doped graphene as catalyst in non-aqueous lithium-oxygen (Li-O<sub>2</sub>) batteries. It was observed that B-doped graphene is a better catalyst for both the oxygen reduction reaction (ORR) and oxygen evolution reaction (OER) in non-aqueous Li-O<sub>2</sub> batteries. Tai *et al* (2014) adopted a two stage strategy to co-dope graphene with boron and nitrogen and used it as a metal-free catalyst for the oxygen reduction reaction (ORR). The co-doped graphene was found to show good stability and tolerance for methanol in alkaline media. Wu *et al* (2012) developed a simplified prototype device for high performance all-solid-state super capacitors (ASSSs), based on 3D boron and nitrogen co-doped monolithic grapheme aero-gels (BN-GAs). The resulting ASSSs show high specific capacitance, good rate capability and enhanced energy or power density.

Umrao *et al* (2015) have used microwave assisted route for synthesis of B-N co-doped reduced grapheme oxide (B-N-MRGO) and observed that B-N-MRGO shows high electrical conductivity in comparison to MRGO, B-MRGO and N-MRGOO, which makes it suitable for fabrication of electronic devices and results in better electromagnetic interference (EMI) shielding ability, making it a useful material for construction of aircrafts and in defense industries, communication systems and stealth technology. It was observed that the co-doping of B and N significantly enhances the electrical conductivity of MRGO because N introduces electrons and B provides holes in the system and may form nano junctions inside the material.

Rani and Jindal (2014) have examined the stability and electronic properties of isomers of B/N co-doped graphene for different levels of doping (4% to 24%) at different doping sites by using VASP code. For equal (atomic %) doping of B and N atoms in graphene, they obtained band gap at the Fermi level. High value of cohesive energy obtained by them indicates the stability of the resulting hetero structures. The band gap and stability of the heterostructures investigated by them were found to depend on the doping sites and the material changes character from semi-metal to semi-conductor with increasing percentage of dopants.

Mukherjee and Kaloni (2012) have also investigated the electronic properties of B-doped, N-doped and B/N co-doped graphene by using Quantum Espresso code, keeping doping levels so as to maintain atomic % of C atoms at 25%, 50% and 75%. For co-doped graphene, the band gap was obtained by them at the Fermi level and the relative position of the Fermi level was found to depend on the concentration of dopants.

Schiro *et al* (2016) observed that co-doping of graphene with boron and nitrogen offers the possibility to further

tune the electronic properties of graphene at the atomic level, potentially creating p- and n- type domains in a single carbon sheet and opening a band gap between valence and conduction band in the 2D semimetal. Ci *et al* (2010) have reported synthesis and characterization of large-area atomic layers of h-BNC material, consisting of hybridized, randomly distributed domains of h-BN and C phases, with compositions ranging from pure BN to pure graphene. It was observed that the structural features and band gap of the new material were different from those of graphene and h-BN. The hybrid h-BNC material enables the development of band gap-engineered applications in electronics and optics.

Recently Muhammad *et al* (2017) have also investigated electronic and optical properties of boron and nitrogen co-doped grapheme and observed that BN rings doped graphene structure shows a direct band gap opening, which increases with the increase in the number of BN-rings present in graphene sheet. Also a significant red shift in absorption towards visible region was found to occur and the height of 14 eV energy peak was found to reduce on increasing BN-rings in graphene.

In view of the potential of B and N co-doped graphene for various applications, mentioned as above, and possibility of new-age electronics by using this material, the present research was conducted to investigate electronic structure of B and N co-doped graphene hetero- structure (BNC<sub>2</sub>) obtained for 25% doping level of each of the two dopants (B and N) in graphene, by using WIEN2K code, which has been found to explain very successfully electronic structure of different materials.

### Theory

Pristine graphene is a 2D honeycomb lattice with hexagonal symmetry of space group 191 (p6/mmm). The C-C bonding in 2D graphene is of sp<sup>2</sup> type and the unit cell is a 120° rhombus, containing two carbon atoms at positions (2/3, 1/3, 0) and (1/3, 2/3, 0) and cell dimensions a=b=2.46 Å. For investigating 2D structures with software like WIEN2K, a 3D structure is created by taking C ≥ 10 Å, so as to introduce sufficient vacuum between two layers, to keep interaction between them to be negligibly small.

The prominent symmetry points in the first Brillouin Zone (FBZ) of graphene are taken as  $\Gamma$  (0,0,0), M(1/2,0,0) and K(2/3,1/3,0) and the path for band structure determination is taken as  $\Gamma \rightarrow M \rightarrow K \rightarrow \Gamma$ .

### Method and Computational Details

For obtaining unit cell of monolayer graphene co-doped with boron and nitrogen, a super cell of dimensions 2x2x1 containing 8C atoms is constructed by using WIEN 2K

code (Blaha *et al.*, 2001), which is based on Density Functional Theory (DFT) (Hohenberg and Kohn, 1964). The Perdew- Burke-Ernzerhof (PBE) potential function (Perdew *et al.*, 1996a) is used in this work, to account for the exchange-correlation (EC) interactions in Generalized Gradient Approximation (GGA) (Perdew *et al.*, 1996b). In the supercell so formed, two C-atoms of same symmetry are replaced by two B-atoms and other two C-atoms of the same symmetry are substituted by N-atoms. This gives rise to a material with unit cell containing 25 % B-atoms, 25% N-atoms and 50% C-atoms, the BNC<sub>2</sub> structure. For the minimum energy requirement, the unit cell of BNC<sub>2</sub> material acquires the symmetry of 65(C/mmm) space group, instead of 191 (P6/mmm), observed for pure graphene, and on adding vacuum between two such layers the 3D structure changes from hexagonal to orthorhombic. As a result of this symmetry transformation, the dimensions of the super cell become  $\approx 3.5 \times 2 \times 1$  as compared to that of pristine graphene. The new cell contains a total of 16 atoms, of which 4 are B-atoms, 4 N-atoms and 8 C-atoms and the cell dimensions were found to be  $a=8.5217 \text{ \AA}$ ,  $b=4.9200 \text{ \AA}$  and  $c=10 \text{ \AA}$ , with  $\alpha = \beta = \gamma = 90^\circ$ . For summing on reciprocal lattice points ( $\bar{G}$ ) inside a sphere in K-space,  $RMT * K_{\max}$  was set=7.0 and number of ( $\bar{K}$ ) points was taken=1000.  $G_{\max}$  was taken=14.0 to keep  $G_{\max} > G_{\min}$  and for convergence of results through iterative solution of Schrödinger equation, the convergence limits were set 0.0001 for energy convergence and 0.001 for charge convergence.

## Results and Discussion

The unit cell of graphene co-doped with B and N, to form hetero-structure of the type BNC<sub>2</sub> is shown in Fig.1. The electronic charge distribution for this cell is depicted in Fig. 2(a). From this figure it is apparent that the charge distribution for this material is quite distorted as compared to pristine graphene, due to the presence of the impurity atoms (B and N). The electronic charge gets shifted away from the N-atoms and points towards B-atoms. Also it may be observed from this diagram that for N-N bond the charge distribution points towards the centre of this bond, whereas for N-C bond it points towards a position close to C-atom on that bond. For B-B bond, it is observed that the shifted charge points towards the B-atoms and the charge distribution in between them is almost parallel to the line joining these atoms. Thus, the electron affinity of B-atoms having one valence electron less as compared to C-atoms in graphene, is clearly established. The N-atoms having one valence electron more as compared to C-atoms, therefore show a repelling effect on electronic charge distribution. In other words,

the characteristic features of electronic charge distribution, mentioned as above, may be considered to arise due to the absence of electrons forming  $\pi$  bonds on B-atoms and excess of  $\pi$  electrons on N-atoms, as compared to C-atoms. The above mentioned features of electronic charge distribution are also revealed by the contour plot for this material, shown in Fig 2(b). The 3D plot for electron density, as obtained from the rho plot, is shown in Fig.3. As depicted by the relevant peak heights, this figure also provides a similar electron density distribution as shown by the diagrams of Fig.2.

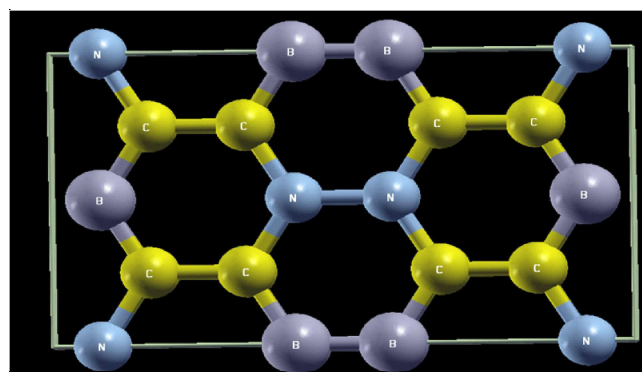


Fig.1. Unit cell of graphene doped with 25 atomic % of Boron and equal atomic % of Nitrogen (BNC<sub>2</sub> hetero structure).

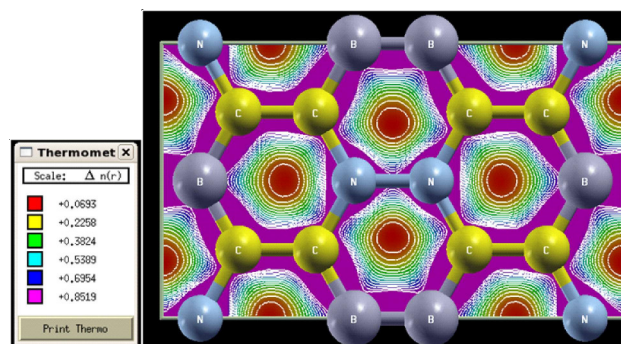


Fig.2. (a). Electron density plot for BNC<sub>2</sub> hetero structure

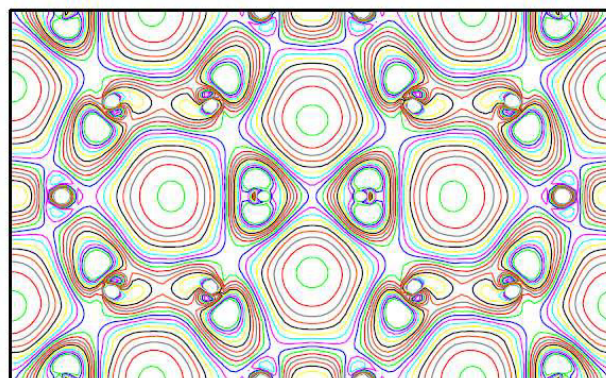
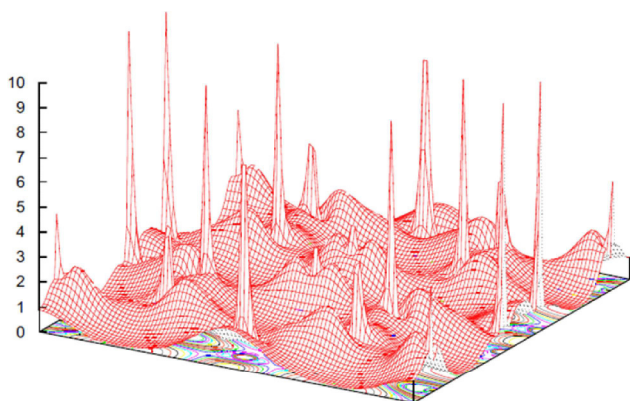


Fig.2. (b). Contour plot for BNC<sub>2</sub> hetero structure.



**Fig.3. Three dimensional picturization of electronic charge distribution in BNC<sub>2</sub> hetero structure, using rho-plot.**

The band structure diagram for the new material BNC<sub>2</sub> is shown in Fig. 4, where the symmetry point  $\Gamma$  has been represented by G. It is revealed by this diagram that the Dirac point, which is obtained at symmetry point K at the Fermi level in pristine graphene and found to shift, along with opening of energy gap, above the Fermi level for B-doping and below the Fermi level for N-doping of graphene (Sharma *et al.*, 2017) is now obtained at the Fermi level. Further, for BNC<sub>2</sub> hetero-structure a band gap opens at symmetry point K and the lines forming the Dirac point in pristine graphene, now become rounded in the vicinity of this point, so that the Dirac like character of electrons vanishes and they now behave as massive particles. Thus, the shifting of Dirac point above/below the Fermi level for B/N doping in graphene, almost cancels out for the co-doped graphene, provided that the doping level (in atomic %) of two types of dopants in graphene is equal. It may also be observed from Fig.4 that for BNC<sub>2</sub> hetero-structure, the Fermi level passes through the band gap, just as in the case of Si. The band gap obtained for this material is about 1.08 eV, which is of the same order as that of Si ( $\approx 1.14$ eV). In BNC<sub>2</sub> the Fermi level divides the energy gap in the ratio of 3.70:1.00 and it lies below the centre of the energy gap, showing p-type behavior of this material. The position of the Fermi level in the band gap can be changed by controlling relative doping of N and B in this material, so as to make it n-type or p-type. Thus, by co-doping with N and B, the characteristics of graphene change from semi-metal to semi-conductor, but with the advantage that the conductivity of graphene is better than that of Si or any other semiconductor, because of the presence of  $\pi$  electrons and holes in it, which can glide freely on the surface of 2D-graphene sheet.

Because of its characteristics, mentioned as above, the new material (BNC<sub>2</sub>) can be used for fabrication of fast speed electronic and optical devices, including switches, giving rise to new age electronics and fast computers.

The present results for band gap of single layer B and N co-doped graphene at 25% doping level ( $\approx 1.08$  eV) are of the same order at K point as reported by Mukherjee and Kaloni (2012) ( $\approx 1.80$  eV) for single layer graphene with 50% C-concentration. However, the position of the Fermi level in the band diagram obtained by them was above the centre of the gap, showing n-type character of the material, whereas in the present case the Fermi level lies below the centre of the band gap, showing p-type character of the material. Also the present results are in qualitative agreement with the experimental result of Ci *et al* (2010) who reported band gap of 1.62 eV for 65 atomic% of C in doped graphene. The present results for band gap of BNC<sub>2</sub> at K point are also in excellent agreement with the theoretical results reported by Rani and Jindal (2013) i.e., 1.06 to 1.08 eV for different configurations of 24% co-doping of B and N in graphene. The opening of band gap for BNC<sub>2</sub> hetero-structure at the Fermi level may be considered to be a consequence of B, N and C hybridization in this material and symmetry breaking due to different core sizes and different electronic structure of B and N atoms, as compared to C-atoms. The band gap at other symmetry points also provides useful information about the material. In the present case the band gap for BNC<sub>2</sub> hetero-structure at symmetry point  $\Gamma$  is found to be 2.21 eV and at the symmetry point M, the energy gap is observed to be 3.66 eV, as shown in Fig. 4.

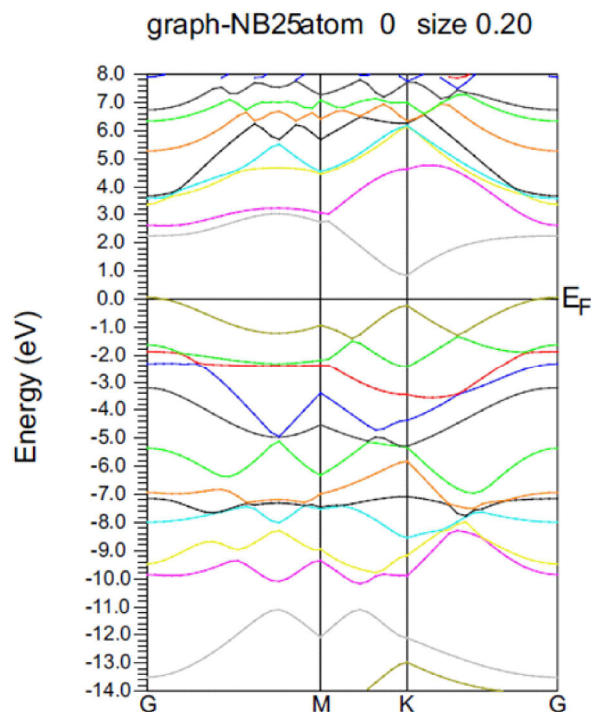
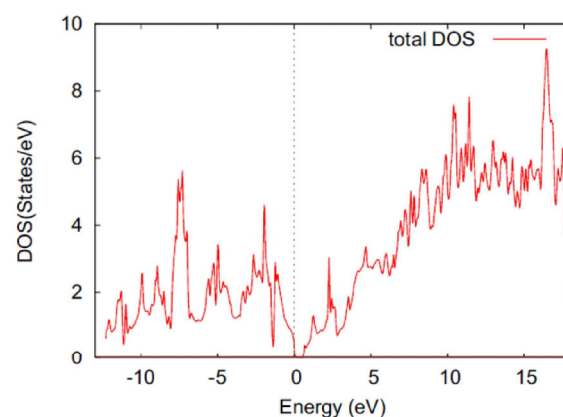


**Fig.4. Band structure of BNC<sub>2</sub> hetero structure.**

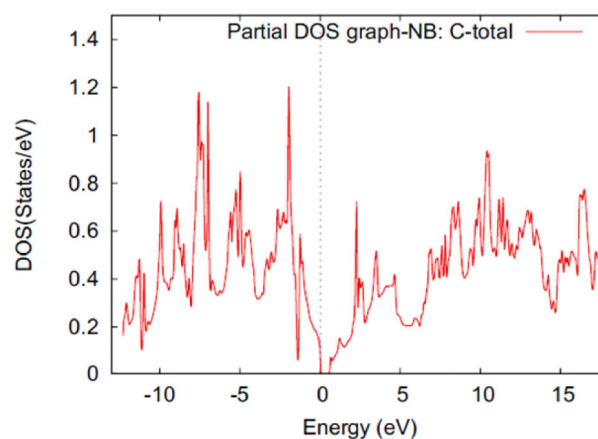
**Table 1. Density of States (states/eV) and corresponding Energy (eV) values at prominent peaks for BNC<sub>2</sub> hetero structure in the DOS spectra**

Sr. No.	Total DOS		Partial DOS					
	Energy (eV)	DOS (states/eV)	C-atom		B-atom		N-atom	
			Energy (eV)	DOS (states/eV)	Energy (eV)	DOS (states/eV)	Energy (eV)	DOS (states/eV)
1.	-11.26	2.05	-11.29	0.50	-11.0	0.16	-11.33	0.63
2.	-9.95	2.59	-9.92	0.73	-10.0	0.16	-9.95	0.47
3.	-8.91	2.89	-8.95	0.70	-8.93	0.24	-8.98	0.56
4.	-7.58	5.41	-7.58	1.19	-7.61	0.25	-7.28	1.58
5.	-7.29	5.62	-6.95	1.14	-6.96	0.19	-	-
6.	-4.98	3.43	-4.98	0.85	-5.42	0.28	-4.98	0.43
7.	-2.67	3.19	-2.66	0.69	-2.67	0.37	-2.67	0.26
8.	-1.95	4.59	-1.94	1.21	-1.70	0.41	-1.97	0.40
9.	-1.21	2.92	-1.21	0.59	-1.21	0.57	-1.29	0.26
10.	+1.24	1.35	+1.24	0.16	+2.26	0.16	+1.26	0.39
11.	+2.25	3.03	+2.26	0.72	+3.56	0.09	2.26	0.25
12.	+3.51	1.87	+3.54	0.53	+6.88	0.11	4.69	0.72
13.	+4.64	3.41	+4.63	0.43	+8.66	0.15	+8.25	0.66
14.	+8.32	5.68	+8.31	0.71	+10.44	0.39	+8.61	0.64
15.	+8.57	5.70	+8.63	0.72	+11.41	0.25	+9.95	0.47
16.	+10.33	7.68	+10.40	0.94	-	-	+10.44	0.49
17.	+11.37	7.79	+11.46	0.74	-	-	+11.17	0.51
18.	+12.98	6.96	+13.17	0.70	+16.50	0.30		
19.	+16.41	9.25	+16.46	0.79	+17.48	0.38	16.42	0.31

The Density of States (DOS) v/s Energy diagrams for the new material are shown in Figures 5(a) to 5(d). Whereas Fig. 5(a) represents the total DOS plot for BNC<sub>2</sub>, figures 5(b) to 5(d) depict the partial DOS plots, illustrating contributions of C, B and N atoms respectively to the total DOS. The values of total DOS and partial DOS due to C, B and N atoms corresponding to prominent peaks in these diagrams are shown in Table 1. It may be observed from this table that the positions of prominent peaks for total DOS match closely with those of partial DOS for C, B and N atoms in this material. However, for matching total DOS with the sum total of partial DOS of different atoms at a particular energy, the contribution of interstitials should also be taken in to consideration. Further, it may be noted from this table that the prominent peaks of total DOS lie in the higher energy range between 8.0 and 16.5eV and in the lower energy range between -7.0 and -8.0 eV. The contribution of C-atoms to DOS in the BNC<sub>2</sub> system is more prominent at -1.94 eV and also at -6.95 and -7.58 eV. On the other hand, the contribution of B-atoms to DOS is found to be comparatively low in whole of the energy range, whereas the contribution made by N-atoms to DOS is quite prominent at -7.28 eV.



(a)



(b)

**Table 2. Density of States (DOS) gap and position of the centre of the gap on energy scale in BNC<sub>2</sub> hetero structure**

For total DOS curve		Width of DOS gap (eV)	Center of DOS gap(eV)
		0.53	0.36
For partial DOS curves:	DOS curve for C-atom	0.51	0.37
	DOS curve for B-atom	0.48	0.32
	DOS curve for N-atom	0.56	0.28

**Table 3. Cell parameter (a and b) dependence of Fermi energy, band gap and DOS gap (depth of vacuum (c=10Å) kept constant)**

% variation in cell parameters (a and b) of parent lattice of pristine graphene	Cell parameters of B and N co-doped graphene		Fermi Energy, E <sub>F</sub> (in eV)	Band Structure			Density of States	
	a (in Å)	b (in Å)		Band gap at K point (eV)	Position of Fermi level w.r.to. centre of band gap (eV)	Band gap at Γ point (eV)	DOS gap (eV)	Position of the centre of DOS gap (eV)
+3%	8.7773	5.0676	-0.1174	1.04	-0.26	2.29	0.51	0.26
+2%	8.6921	5.0183	-0.1088	1.04	-0.26	2.26	0.51	0.26
+1%	8.6069	4.9691	-0.1014	1.04	-0.26	2.24	0.55	0.33
+0%	8.5217	4.9200	-0.0964	1.08	-0.31	2.21	0.55	0.34
-1%	8.4364	4.8708	-0.0814	1.04	-0.21	2.14	0.55	0.28
-2%	8.3512	4.8215	-0.0722	1.09	-0.24	2.10	0.44	0.27
-3%	8.2660	4.7723	-0.0598	1.09	-0.24	2.06	0.38	0.30

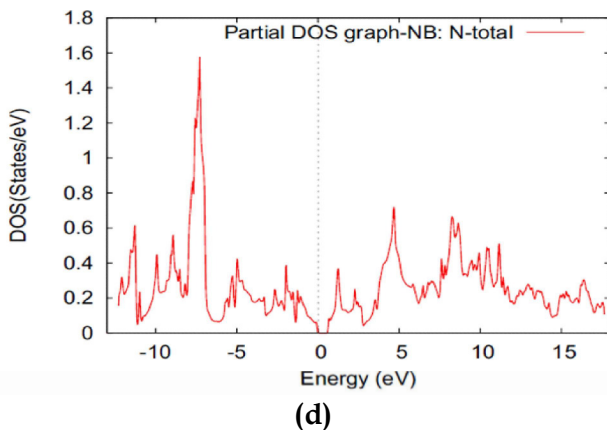
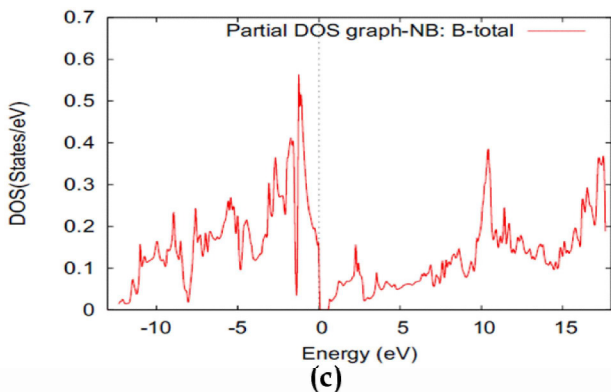


**Fig.5. Density of states (DOS) v/s Energy diagrams for BNC<sub>2</sub> hetero structure: (a) total Density of States; (b) Partial DOS for atom C; (c) Partial DOS for atom B, and (d) Partial DOS for atom N.**

It may also be observed from figures 5(a) to 5(d) that now zero DOS states occur near the Fermi level in all the cases. The width of the DOS gap and position of the centre of the gap for the four cases are shown in Table 2. It may be observed from this table that the DOS gap for the total DOS (0.53 eV) is nearly equal to the average of the DOS gaps for the three types of atoms in the system. The centre of the DOS gap in the above mentioned cases lie very close to the Fermi level, showing that the opening of the band gap in this material will be very close to the Fermi surface and hence the material will behave as a semiconductor.

Further, the effect of cell parameter variation on the energy bands and Density of States was also examined in the present work. The relevant data is assembled in Table 3. From this table, it may be observed that on changing cell parameters (a and b) from +3% to -3% of their pristine values (keeping c=10Å<sup>0</sup> constant), the Fermi energy increases from -0.1174 to -0.0598 eV. The band gap at symmetry point G is found to decrease from 2.29 eV to 2.06 eV as we change the cell parameters a and b from +3% to -3%. The band gap at K point and position of Fermi level with respect to centre of the gap are, however, not so sensitive to the variation of cell parameters. The band gap at K point is found to slightly increase when the cell parameters are decreased, whereas on increasing the cell parameters the band gap at this symmetry point is found to slightly decrease. On the other hand, the position of the Fermi surface is found to be below the centre of band gap, showing p-type character of the material, for all values of cell parameters (i.e., within the limits from +3% to -3%).

The table also reveals that the DOS gap decreases more rapidly for reduction in the cell parameters as compared to its values for increase in the cell parameters. The position of the centre of DOS gap is found to be positive in all cases (i.e., for variation of cell parameters from +3% to -3%), showing that the DOS gap lies just above the Fermi level.

## Conclusion

By doping graphene simultaneously with B and N with equal atomic % of the two dopants (25% each in the present case, forming BNC<sub>2</sub> hetero structure), a band gap of about 1eV opens and the Fermi level passes through the band gap, as in case of Si. The presence of  $\pi$  electrons and holes on the surface of the co-doped graphene sheet contributes to high electrical conductivity in this material, thus making it suitable for fabrication of high speed electronic and optical devices. The hetero structure BNC<sub>2</sub>, therefore, has a potential for development of new-age 2D electronics and replace Si-based technology presently being used for fabrication of electronic devices.

## Acknowledgements

The authors acknowledge with thanks the computational facilities for this work provided by the Inter University Accelerator Centre (IUAC), Delhi at their High Performance computing system. The Authors gratefully acknowledge the technical support provided by Prof. R. K. Sharma, Bikaner for many useful discussions regarding this work. Facilities extended by the IIS University and MNIT Jaipur for this work are also gratefully acknowledged.

## References

- Blaha, P., Schwarz, K., Madsen, G. K. H., Kvasnicka, D., Liutz, J. (2001) WIEN2K: An augmented plane wave plus local orbital program for calculating crystal properties. KasheingSchwarz, Techn. University: Austria.
- Choi, H.J., Jung, S.M., Seo, J. M., Chang, D.W., Dai, L., Baek, J.B. (2012) Graphene for energy conversion and storage in fuel cells and super capacitors. *Nano Energy* **1**:534-551. doi:10.1016/j.nanoen.2012.05.001
- Ci, L., Song, L., Jin, C., Jariwala, D., Wu, D., Li, Y., Srivastava, A., Wang, Z. F., Storr, K., Balicas, L., Liu, F., Ajayan, P. M. (2010) Atomic layers of hybridized boron nitride and graphene domains. *Nat Mater* **9**:430-435. doi: 10.1038/nmat2711
- Fujimoto, Y. (2015) Formation, Energetics and Electronic properties of graphene monolayer and bilayer doped with hetero atoms. *Adv Cond Matter Phys* 2015571490-pp-1-14. doi:10.1155/2015/571490
- Guo, B., Fang, L., Zhang, B., Gong, J. R. (2011) Graphene doping: & review. *Insciences J* **1**:80-89. doi:10.5640/insc.010280
- Hohenberg, P., Kohn, W. (1964) Inhomogeneous electron gas. *Phys Rev* **136**: B864-B871.
- Jiang, H.R., Zhao, T.S., Shi, L., Tan, P., An, L. (2016) First principles study of Nitrogen-, Boron-doped graphene and co-doped graphene as the potential catalysis in non-aqueous Li-O<sub>2</sub> batteries. *J Phys Chem C* **120**:6612-6618. doi: 10.1021/acs.jpcc.6b00136
- Joucken, F., Tison, Y., Lagoüte, J., Dumont, J., Cabosart, D., Zheng, B., Repain, V., Chacon, C., Girard, Y., Botello-Méndez, A. R., Rousset, S., Sporcken, R., Charlier, J. C., Henrard, L. (2012) Localized state and charge transfer in Nitrogen-doped graphene. *Phys Rev B* **85**:161408-1. doi:10.1103/PhysRevB.85.161408
- Liu, J., Xue, Y., Zhang, M., Dai, L. (2012) Graphene-based materials for energy application. *MRS Bulletin* **37**:1265-1272. doi: 10.1557/mrs.2012.179
- Muhammad, R., Shuai, Y., He-Ping, T. (2017) First-principles study of electronic and optical properties of boron and nitrogen doped graphene. *Proc AIP Conf* 1846 030002; doi: 10.1063/1.4983600
- Mukherjee, S., Kaloni, T.P. (2012) Electronic properties of boron- and nitrogen- doped graphene: a first principle study. *J Nanopart Res* **14**:1059-1063. doi:10.1007/s11051-012-1059-2
- Novoselov, K.S., Geim, A.K., Morozov, S.V., Jiang, D., Zhang, Y., Dubonos, S.V., Grigorieva, I.V., Firsov, A.A. (2004) Electrical field effect in atomically thin carbon films. *Science* **306**:666-669. doi:10.1126/science.1102896
- Panchakarla, L.S., Subrahmanyam, K.S., Saha, S.K., Govindaraj, A., Krishnamurthy, H. R., Waghmare, U. V., Rao, C.N.R. (2009) C.N.R. Synthesis, structure and properties of Boron and Nitrogen doped graphene. *Adv Mater* **21**:4726-4730. doi:10.1002/adma.200901285
- Perdew, J.P., Burke, K., Wang, Y. (1996a) Generalized gradient approximation for the exchange-correlation hole of a many-electron system. *Phys Rev B* **54**:16533-16539

- Perdew, J.P., Burke, K., Ernzerhof, M. (1996b) Generalized gradient approximation made simple. *Phys Rev Lett* **77**:3865-3368. doi:10.1103/PhysRevLett.77.3865
- Ramchandran, R., Mani, V., Chen, S.M., Saraswathi, R., Lou, B.S. (2013) Recent trends in graphene based electrode materials for energy storage devices and sensor application. *Int J ElectrocheSci* **8**:11680-11694
- Rani, P., Jindal, V.K. (2014) Stability and electronic properties of isomers of B/N co-doped graphene. *Applied Nanoscience* **4**:989-996. doi:10.1038/srep19115
- Rani, P., Jindal, V.K. (2013) Designing band gap of graphene by B- and N- dopant atoms. *RSC Adv* **3**:802-812. doi: 10.1039/C2RA22664B
- Schiros, T., Nordlund, D., Palova, L., Zhao, L., Levendorf, M., Jaye, C., Reichman, D., Park, J., Hybertsen, M., Pasupathy, A. (2016) Atomistic Interrogation of B-N co-dopant structure and their Electronic effects in Graphene. *ACS Nano* **10**:6574-6584. doi: 10.1021/acsnano.6b01318
- Sharma, R., Khan, S., Goyal, V., Sharma, V., Sharma, K.S. (2017) Investigation on effect of Boron and Nitrogen substitution on electronic structure of graphene. *Flat Chem* **1**:20-33. doi:10.1016/j.flatc.2016.10.001
- Tai, J., Hu, J., Chen, Z., Lu, H. (2014) Two-step synthesis of boron and nitrogen co-doped graphene as a synergistically enhanced catalyst for the oxygen reduction reaction. *RSC Adv* **4** :61437-61443. doi: 10.1039/C4RA10162F
- Tokarev, A., Avdeenkov, A. V., Langmi, H., Bessarabov, D.G. (2015) Bessarabov, D.G. Modeling hydrogen storage in boron substituted graphene decorated with potassium metal atom. *Int J Energy Res* **39**:524-528. doi: 10.1002/er.3268
- Umrao, S., Gupta, T.K., Kumar, S., Singh, V. K., Sultania, M.K., Jung, J. H., Oh, I.K., Srivastava, A. (2015) Microwave-Assisted Synthesis of Boron and Nitrogen co-doped Reduced graphene oxide for the protection of Electromagnetic Radiation in Ku-band. *ACS Appl Mater Interfaces* **7**:19831-19842. doi: 10.1021/acsami.5b05890
- Wang, H., Maiyalagan, T., Wang, X. (2012) Review on recent programme in nitrogen-doped graphene: synthesis, characterization and its potential application. *ACS Catal* **2**:781-794. doi: 10.1021/cs200652y
- Wu, Z., Winter, A., Chen, L., Sun, Y., Turchanin, A., Feng, X., Muellen, K. (2012) Three-Dimensional nitrogen and boron co-doped graphene for high-performance all-solid-state supercapacitors. *Adv Mater* **24**:5130-5133. doi:10.1002/adma.201201948
- Zhu, J., Yang, D., Yin, Z., Yan, Q., Zhang, H. (2014) Graphene and grapheme based materials for energy storage applications. *Small* **10**:3480-3496. doi: 10.1002/sml.201303202